

Differential Stabilities and Sequence-Dependent Base Pair Opening Dynamics of Watson–Crick Base Pairs with 5-Hydroxymethylcytosine, 5-Formylcytosine, or 5-Carboxylcytosine

Marta W. Szulik,[†] Pradeep S. Pallan,[‡] Boguslaw Nocek,[§] Markus Voehler,[†] Surajit Banerjee,^{||} Sonja Brooks,[⊥] Andrzej Joachimiak,[§] Martin Egli,[‡] Brandt F. Eichman,[⊥] and Michael P. Stone^{*,†}

[†]Department of Chemistry, Vanderbilt Institute of Chemical Biology, Vanderbilt Ingram Cancer Center, and Center for Structural Biology, Vanderbilt University, Nashville, Tennessee 37235, United States

[‡]Department of Biochemistry, Vanderbilt Institute of Chemical Biology, Vanderbilt Ingram Cancer Center, and Center for Structural Biology, School of Medicine, Vanderbilt University, Nashville, Tennessee 37232, United States

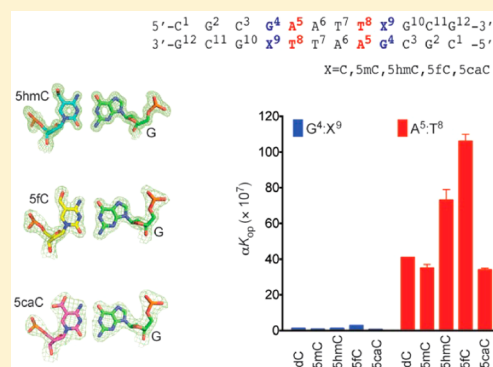
[§]Bioscience Division, Argonne National Laboratory, Argonne, Illinois 60439, United States

^{||}Northeastern Collaborative Access Team and Department of Chemistry and Chemical Biology, Cornell University, Argonne National Laboratory, Argonne, Illinois 60439, United States

[⊥]Department of Biological Sciences, Vanderbilt Institute of Chemical Biology, and Center for Structural Biology, Vanderbilt University, Nashville, Tennessee 37235, United States

Supporting Information

ABSTRACT: 5-Hydroxymethylcytosine (5hmC), 5-formylcytosine (5fC), and 5-carboxylcytosine (5caC) form during active demethylation of 5-methylcytosine (5mC) and are implicated in epigenetic regulation of the genome. They are differentially processed by thymine DNA glycosylase (TDG), an enzyme involved in active demethylation of 5mC. Three modified Dickerson–Drew dodecamer (DDD) sequences, amenable to crystallographic and spectroscopic analyses and containing the 5′-CG-3′ sequence associated with genomic cytosine methylation, containing 5hmC, 5fC, or 5caC placed site-specifically into the 5′-T⁸X⁹G¹⁰-3′ sequence of the DDD, were compared. The presence of 5caC at the X⁹ base increased the stability of the DDD, whereas 5hmC or 5fC did not. Both 5hmC and 5fC increased imino proton exchange rates and calculated rate constants for base pair opening at the neighboring base pair A⁵:T⁸, whereas 5caC did not. At the oxidized base pair G⁴:X⁹, 5fC exhibited an increase in the imino proton exchange rate and the calculated k_{op} . In all cases, minimal effects to imino proton exchange rates occurred at the neighboring base pair C³:G¹⁰. No evidence was observed for imino tautomerization, accompanied by wobble base pairing, for 5hmC, 5fC, or 5caC when positioned at base pair G⁴:X⁹; each favored Watson–Crick base pairing. However, both 5fC and 5caC exhibited intranucleobase hydrogen bonding between their formyl or carboxyl oxygens, respectively, and the adjacent cytosine N⁴ exocyclic amines. The lesion-specific differences observed in the DDD may be implicated in recognition of 5hmC, 5fC, or 5caC in DNA by TDG. However, they do not correlate with differential excision of 5hmC, 5fC, or 5caC by TDG, which may be mediated by differences in transition states of the enzyme-bound complexes.



Cytosine methylation by DNA methyltransferases^{1–4} to form 5-methylcytosine (5mC)⁵ is important in epigenetic regulation of the eukaryotic genome.^{6,7} The reconversion of 5mC to cytosine during active demethylation^{8–25} involves the stepwise oxidation of 5mC. Oxidation of 5mC to 5-hydroxymethylcytosine (5hmC)^{10,26,27} is accomplished by ten-eleven translocation (TET) dioxygenases^{15,28–30} and occurs in response to oxidative stress as a consequence of UV radiation.³¹ Further oxidation of 5hmC by TET dioxygenases forms 5-formylcytosine (5fC)²⁷ and 5-carboxylcytosine (5caC).^{8,22,27–30,32} These have been detected in cellular DNA.^{32,33} Both 5fC and 5caC, but not 5hmC, are substrates for thymine DNA glycosylase (TDG),¹⁴ consistent

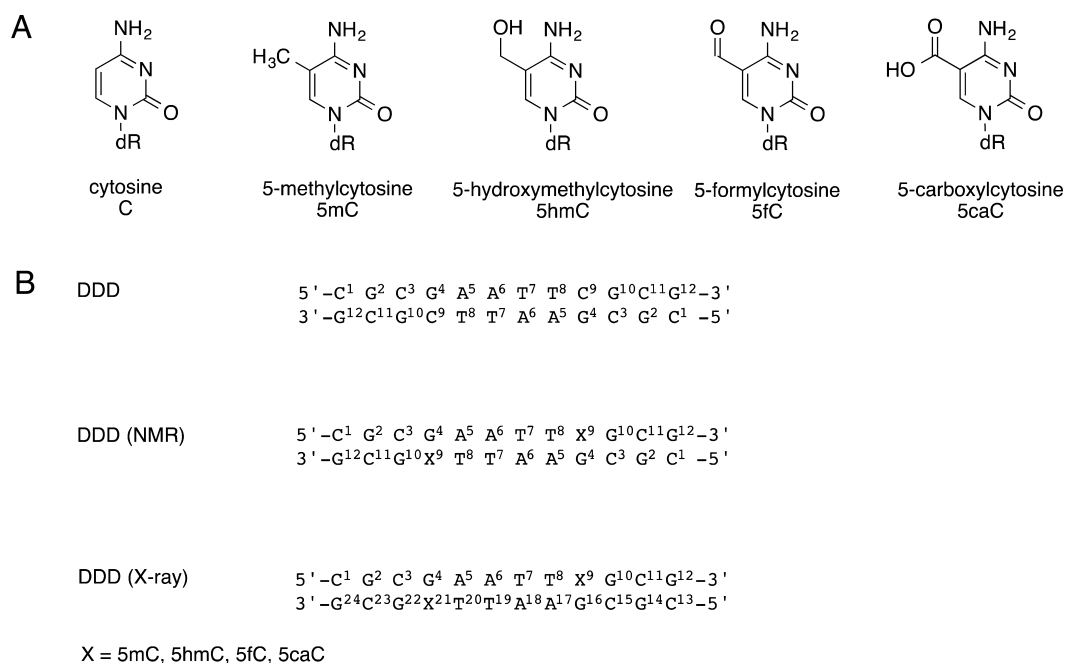
with the greater abundance of 5hmC in mammalian tissues⁹ and implicating catalyzed base excision of oxidized 5mC derivatives in active demethylation.

The differential processing of 5fC and 5caC vs 5hmC by TDG could be mediated by their differential recognition in DNA. Recently, Raiber et al.³⁴ reported that a DNA dodecamer containing three 5fC sites in an iterated CG repeat sequence exhibited 5fC-specific helical unwinding, due to specific changes in the geometry of the grooves and base pairs involving 5fC.

Received: December 17, 2014

Published: January 29, 2015

Chart 1. (A) Structures of C, 5mC, 5hmC, 5fC, and 5caC and (B) Sequences and Numbering of the Nucleotides for DDD and Oxidized DDD Duplexes^a



^aIn solution, the two strands of the DDD exhibit pseudo-dyad symmetry. NMR resonances of symmetry-related nucleotides in the two strands are not individually observed. In the crystal, corresponding nucleotides from paired strands are not symmetry-related, and nucleotides are numbered individually. DDD^m, DDD^{hm}, DDD^f, and DDD^{ca} refer to the DDD containing 5mC, 5hmC, 5fC, and 5caC, respectively.

DNA glycosylases may also exploit differential base pair opening rates as a basis for substrate recognition. For example, enhanced base pair opening rates at A:U base pairs facilitate the recognition of uracil by uracil DNA glycosylase (UDG).³⁵ It has also been hypothesized that TDG recognizes wobble base pairing geometry at oxidized cytosines,^{17,19,23,36,37} as the imino tautomers of 5caC or 5fC may adopt wobble-like base pairs with the complementary G.^{20,37} However, calculations of the stabilities of the amino and imino tautomers of 5fC and 5caC at the nucleobase level have suggested that, when paired with G, both 5fC and 5caC, which are substrates for TDG,¹⁴ preferentially form Watson-Crick pairs.²³ Alternatively, as proposed by Maiti et al.,¹⁴ the differential processing by TDG could be mediated by differences in the corresponding transition state catalytic complexes involving 5fC, 5caC, or 5hmC. Maiti et al.¹⁴ proposed that the preferential excision of 5fC and 5caC by TDG is facilitated by the presence of electron-withdrawing substituents at the C5 carbon for these two oxidized cytosines. This electron-withdrawing effect^{14,23} would be anticipated to stabilize developing negative charge in the transition state complex for base excision.

Here, we have incorporated 5hmC, 5fC, or 5caC into the 5'-T⁸X⁹G¹⁰-3' sequence of the self-complementary Dickerson-Drew dodecamer (DDD),^{38,39} which contains the 5'-CG-3' sequence associated with genomic cytosine methylation, forming DDD^{hm}, DDD^f, and DDD^{ca} duplexes (Chart 1), respectively. Importantly, the DDD is amenable to crystallographic³⁸⁻⁴³ and spectroscopic⁴⁴⁻⁴⁷ analyses. The characterization of the DDD^{hm}, DDD^f, and DDD^{ca} duplexes by thermal melting studies, measurements of base pair opening dynamics, crystallography, and NMR reveals lesion- and sequence-specific differences among 5hmC, 5fC, or 5caC in the 5'-T⁸X⁹G¹⁰-3' sequence, which may be relevant to their recognition by TDG. Relative to 5hmC and 5fC, incorporation of 5caC increases the

stability of the DDD. This is reflected in reduced base pair opening dynamics for DDD^{ca}, as compared to that for DDD^{hm} and DDD^f, at neighboring base pair A⁵:T⁸. Similar, but smaller, differences in base pair opening dynamics are observed at the oxidized base pair G⁴:X⁹, whereas minimal effects are observed at neighboring base pair C³:G¹⁰. No evidence for wobble base pairing interactions involving the oxidized cytosines is observed; each of these oxidized cytosines favors Watson-Crick base pairing. These sequence-specific differences in the DDD may be related to the recognition of these oxidized cytosines by TDG. However, they differ from the sequence-specific effects observed by Raiber et al.³⁴ for an iterated CG repeat containing three 5fC sites. Moreover, they do not correlate with the differential ability of TDG to excise 5fC and 5caC vs 5hmC,¹⁴ which may be mediated by differences in the transition state complex for base excision.

EXPERIMENTAL PROCEDURES

Oligodeoxynucleotide Synthesis. Oligodeoxynucleotides were synthesized by Midland Certified Reagent Co. (Midland, TX) and purified by anion-exchange HPLC. The DDD^{hm} duplex was prepared with an Expedite 8909 DNA synthesizer (PerSeptive Biosystems) on a 1 μmol scale using ethylcyanide-protected 5-hydroxymethyl-dC, phenoxyacetyl-protected dA, 4-isopropyl-phenoxyacetyl-protected dG, acetyl-protected dC, and dT phosphoramidites and solid supports (Glen Research, Inc., Sterling, VA). The modified phosphoramidite was incorporated by removing the column from the synthesizer and sealing it with two syringes, one of which contained 250–300 μL of the manufacturer's ¹H-tetrazole activator solution (1.9–4.0% in CH₃CN, v/v) and the other contained 250 μL of the modified phosphoramidite solution (15 mg in anhydrous CH₃CN). The ¹H-tetrazole and the phosphoramidite solutions

were sequentially drawn through the column (¹H-tetrazole first), and this procedure was repeated over 30 min. The column was washed with anhydrous CH₃CN and returned to the synthesizer for capping, oxidation, and detritylation steps. The deprotection was accomplished with 30% NH₄OH for 17 h at 75 °C.

Oligodeoxynucleotide Purification and Characterization. Oligodeoxynucleotides were purified by semipreparative HPLC at 260 nm (Atlantis, Waters Corporation, C18, 5 μm, 250 mm × 10.0 mm). The column was equilibrated either with 30 mM sodium phosphate (pH 7.0) (for DDD^m, DDD^{hm}, DDD^{ca}) or 0.1 M ammonium formate (pH 6.5) (for DDD^f). The gradient was 1–15% CH₃CN over 20 min, 15–80% CH₃CN over 5 min, and 1% CH₃CN over 5 min, at 4.5 mL/min. Oligodeoxynucleotides were desalted by passing over G-25 Sephadex (GE Healthcare, Little Chalfont, Buckinghamshire, UK). Oligodeoxynucleotides were characterized by MALDI-TOF mass spectrometry (calcd for DDD [M – H][–] *m/z* 3646.4, found *m/z* 3647.8; calcd for DDD^m [M – H][–] *m/z* 3660.5, found 3663.4; calcd for DDD^{hm} [M – H][–] *m/z* 3675.5, found 3679.7; calcd for DDD^f [M – H][–] *m/z* 3674.4, found 3673.2; calcd for DDD^{ca} [M – H][–] *m/z* 3690.4, found 3693.1). Oligodeoxynucleotides were prepared in 100 mM NaCl, 50 μM Na₂EDTA, in 10 mM sodium phosphate (pH 7.0), heated at 85 °C for 15 min, and annealed by cooling to room temperature. Duplex concentrations were determined by UV absorbance, using extinction coefficients calculated at 260 nm.⁴⁸

Thermal Denaturation. The concentration of DNA was 1.2 μM. Measurements were conducted in 100 mM NaCl, 50 μM Na₂EDTA, in 10 mM sodium phosphate (pH 7.0). The temperature was increased from 10 to 80 °C at 1 °C/min. *T_m* values were calculated from first-order derivatives of 260 nm absorbance vs temperature profiles.⁴⁹

NMR. Spectra were obtained at 900 MHz using a 5 mm cryogenic probe (Bruker Biospin Inc., Billerica, MA). Oligodeoxynucleotides were prepared at a duplex concentration of 0.25 mM in 180 μL of 100 mM NaCl, 50 μM Na₂EDTA, 11 mM NaN₃, in 10 mM sodium phosphate (pH 7.0). The samples were exchanged with D₂O and dissolved in 180 μL of 99.996% D₂O to observe nonexchangeable protons. NOESY⁵⁰ spectra were collected in 99.996% D₂O to observe nonexchangeable protons. The temperature was 15 °C. TPPI quadrature detection was used, and data were collected at a mixing time of 250 ms. The relaxation delay was 2.0 s. Data were recorded with 2k real points in the *t2* dimension and 1k real points in the *t1* dimension. Spectra were zero-filled during processing to create a 2k × 2k matrix. Chemical shifts were referenced to the chemical shift of water at the corresponding temperature, with respect to 4,4-dimethyl-4-silapentane-1-sulfonic acid (DSS). To observe exchangeable protons, samples were prepared in 9:1 H₂O/D₂O. For observation of imino protons, spectra were recorded at 5, 15, 25, 35, 45, and 55 °C. NOESY spectra were collected at 5 °C with 70 or 250 ms mixing times and relaxation delay of 2.0 s. Water suppression was achieved by the Watergate pulse sequence.⁵¹ Data were processed with TOPSPIN (2.0.b.6, Bruker Biospin Inc., Billerica, MA).

Base Pair Opening. NMR data were collected at 500 MHz using a 5 mm cryogenic probe, at 15 °C. Samples were in 180 μL of 9:1 H₂O/D₂O containing 100 mM NaCl, 50 μM Na₂EDTA, 11 mM NaN₃, 1 mM triethanolamine, in 10 mM sodium phosphate (pH 8.9).^{52–56} The presence of triethanol-

amine enabled the pH of the sample to be monitored during the titration, *in situ*, by measuring the chemical shift difference between the two methylene groups.⁵² Magnetization transfer from water to the imino protons was followed by observation of the imino proton resonances after variable mixing times.^{57,58} Selective spin inversion of the water protons was achieved with a 2 ms 180° sinc pulse with 1000 points. To minimize effects of radiation damping during the mixing time, a 0.1 G cm^{–1} gradient was used. Water suppression was achieved by a binomial 1–1 echo sequence, jump and return,⁵⁹ with flanking 1 ms smooth square shape gradients, 15 G cm^{–1}. Sixteen values of the delay ranging from 1 ms to 15 s were used. Data were processed in TOPSPIN. Ammonia, *pK_a* of 9.2 at 15 °C, was the proton acceptor.⁵⁷ Data analyses were performed using PRISM (v. 6.0b, GraphPad Software, Inc., La Jolla, CA). Exchange rates were calculated using established methods.^{60,61} In order to determine rates of base pair opening, exchange rates were plotted against concentrations of the active form of the ammonia base catalyst. Equilibrium constants for base pair opening were calculated by fitting exchange rate data as a function of ammonia concentration.⁵²

Crystallization and X-ray Diffraction. Crystals were grown at 18 °C over 8 to 16 days by hanging-drop vapor diffusion, using the nucleic acid mini-screen (Hampton Research, Aliso Viejo, CA). Droplets of 2 μL containing 1.2 mM duplex in precipitant solution were equilibrated against 0.75 μL of 35% MPD. The solution compositions are summarized in Table S1 in the Supporting Information. Single crystals were mounted in nylon loops and flash-frozen in liquid nitrogen.

For DDD^{hm}, data were collected on the 19-ID beamline of the Structural Biology Center at the Advanced Photon Source (APS) of Argonne National Laboratory (ANL, Argonne, IL).⁶² The wavelength was 0.9794 Å. Initial indexing and scaling of diffraction images and further reflection merging was done using HKL3000.⁶³ To ensure completeness of the data, two passes were collected. For DDD^{ca}, data were collected on the 24-IDC beamline of the Northeastern Collaborative Access Team (NE-CAT) at the APS (ANL). The wavelength was 0.97920 Å. Initial indexing and scaling of diffraction images, together with reflection merging, were done using XDS^{64,65} and SCALA⁶⁶ in the CCP4⁶⁷ suite as part of the RAPD data collection strategy at NE-CAT. For DDD^f, data were collected on the 21-IDD beamline of the Life-Sciences Collaborative Access Team (LS-CAT) at the APS (ANL). The wavelength was 1.000 Å. Initial indexing and scaling of diffraction images, together with reflection merging were done in HKL2000.⁶⁸ Details are shown in Table 1.

Crystal Structure Determination and Refinement. Structures were determined by molecular replacement using the DDD as the search model (PDB ID code 436D).⁴⁰ Molecular replacement searches were completed with MOLREP^{69,70} in the CCP4 suite.⁶⁷ An initial model was checked and rebuilt in COOT.⁷¹ The model was rebuilt and further refined using REFMAC.^{72,73} Final models were refined against all reflections, except for 5% randomly selected reflections used for monitoring *R_{free}*. The refinement statistics are presented in Table 1.

Data Deposition. Complete structure factors and data coordinates were deposited in the Protein Data Bank (<http://pdb.org>): PDB ID code 4I9V for DDD^{hm}, 4QC7 for DDD^f, and 4PWM for DDD^{ca}.

Table 1. Crystal Data, Data Collection, and Refinement Statistics for the DDD^{hm}, DDD^f, and DDD^{ca} Duplexes

parameter	DDD ^{hm}	DDD ^f	DDD ^{ca}
Crystal Data			
space group	<i>P</i> 2 ₁ 2 ₁ 2 ₁	<i>P</i> 2 ₁ 2 ₁ 2 ₁	<i>P</i> 2 ₁ 2 ₁ 2 ₁
Unit Cell			
<i>a</i> (Å)	25.61	25.09	24.25
<i>b</i> (Å)	41.34	41.47	41.34
<i>c</i> (Å)	64.32	65.69	66.41
Data Collection			
resolution range (Å)	40–1.02	35–1.90	26–1.95
no. of unique reflections	37 637	5801	5113
completeness (%)	99.6	99.3	99.5
in the outer shell (%)	98.5	100	97.5
<i>R</i> _{merge} ^a	0.044	0.064	0.045
in the outer shell	0.979	0.738	0.619
<i>I</i> / σ (<i>I</i>)	52	60	16
in the outer shell	1.7	3.3	2.8
Structure Refinement			
resolution range (Å)	40–1.02	35–1.90	26–1.95
<i>R</i> _{work}	0.156	0.226	0.221
<i>R</i> _{free}	0.178	0.245	0.267
RMS Deviation			
bond lengths (Å)	0.014	0.011	0.009
angle distances (deg)	2.4	1.3	2.2
no. of ions	1 Mg ²⁺		
no. of ligands	3		
no. of water molecules	178	17	13

^a $R_{\text{merge}} = \sum_{hkl} \sum_i |I_i - \langle I \rangle| / \sum_{hkl} \sum_i \langle I \rangle$, where *I_i* is the intensity for the *i*th measurement of an equivalent reflection with indices *h*, *k*, and *l*.

RESULTS

Stabilities of the Duplexes Containing Oxidized Cytosines. The impact of placing 5hmC, 5fC, or 5caC site specifically into the 5'-CG-3' sequence was investigated by incorporating each oxidized cytosine into the 5'-T⁸X⁹G¹⁰-3' sequence of the DDD.^{38,39} The *T_m* values of the duplexes were obtained in 100 mM NaCl at pH 7. They were compared to both the unmodified DDD and also to the DDD containing

5mC in the 5'-T⁸X⁹G¹⁰-3' sequence (DDD^m). The *T_m* of the DDD duplex was 48 °C, the *T_m* of the DDD^m duplex was 46 °C, the *T_m* of the DDD^{hm} duplex was 48 °C, and the *T_m* of the DDD^f duplex was 46 °C. These small differences in *T_m* suggested that the presence of 5mC or of the oxidized cytosines 5hmC or 5fC in the 5'-T⁸X⁹G¹⁰-3' sequence did not greatly affect the *T_m* of the DDD. In contrast, the *T_m* of the DDD^{ca} duplex increased to 54 °C. NMR spectra of the exchangeable guanine N1H and thymine N3H imino protons were recorded from 5–55 °C (Figure 1). The resonances were assigned using standard methods.⁷⁴ For the DDD^{ca} duplex, the G⁴ N1H proton remained sharp at 55 °C, consistent with the increased *T_m* value associated with the 5caC nucleobase in the 5'-T⁸X⁹G¹⁰-3' sequence. At the neighbor A⁵:T⁸ base pair, the T⁸ N3H resonance remained detectable at 55 °C, although it exhibited broadening. At the neighbor C³:G¹⁰ base pair, the G³ N1H resonance remained detectable at 55 °C, also exhibiting broadening. The stabilizing effect extended two base pairs in each direction, also including the imino protons of base pairs G²:C¹¹ and A⁶:T⁷. In contrast, for the DDD^{hm} duplex at the oxidized G⁴:X⁹ base pair, the G⁴ N1H resonance was severely broadened at 55 °C. Likewise, the corresponding resonance in the DDD^f duplex was severely broadened at 55 °C. At the neighboring base pair C³:G¹⁰, the G¹⁰ N1H resonance in the DDD^f duplex broadened at 35 °C. The T⁸ N3H resonances broadened at 45 °C in the DDD^f duplex and at 55 °C in the DDD^{hm} duplex. The temperature dependence of line widths of the imino resonances is shown in Figure S1 of the Supporting Information.

Base Pair Opening Dynamics. Magnetization transfer from water after variable times was followed by observation of the guanine N1H and thymine N3H resonances, at 15 °C. The imino proton exchange rates were measured in the absence and the presence of added ammonia base catalyst.^{45,52,57,58,61,75} The exchange with water follows a two-state model, where the base pair undergoes a conformational change from the closed to the open state, from which proton exchange occurs.^{57,75} The open base pair is exchange-competent because the proton is accessible to acceptors in solution. As described by Russu and co-workers,^{75–77} in the EX1 regime, the concentration of

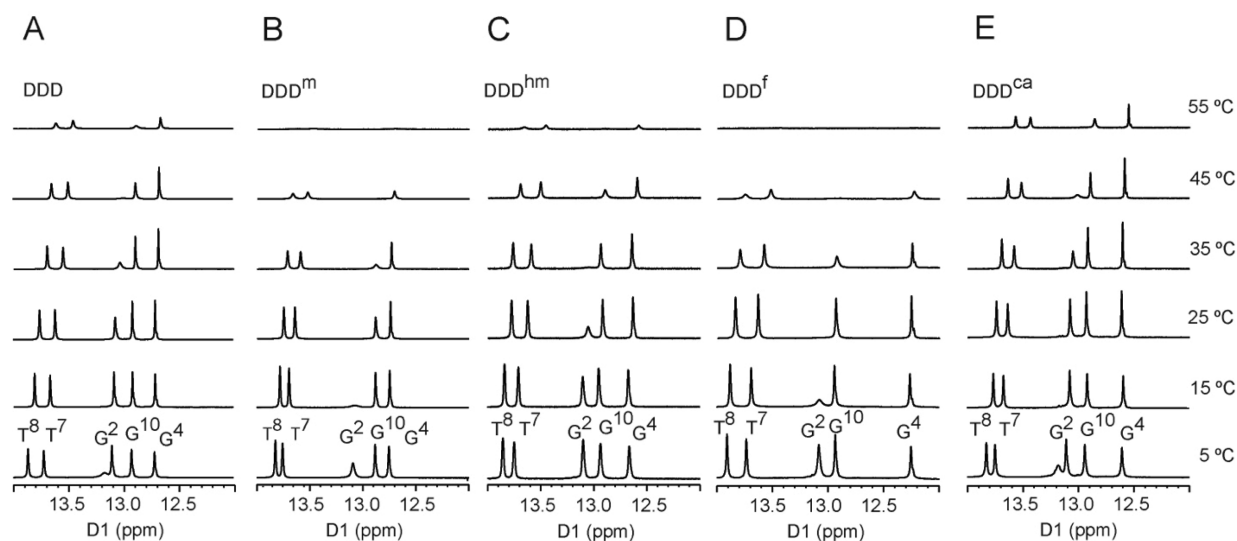


Figure 1. ¹H NMR of imino proton resonances as a function of temperature for (A) DDD, (B) DDD^m, (C) DDD^{hm}, (D) DDD^f, and (E) DDD^{ca}. Data were collected at 900 MHz.

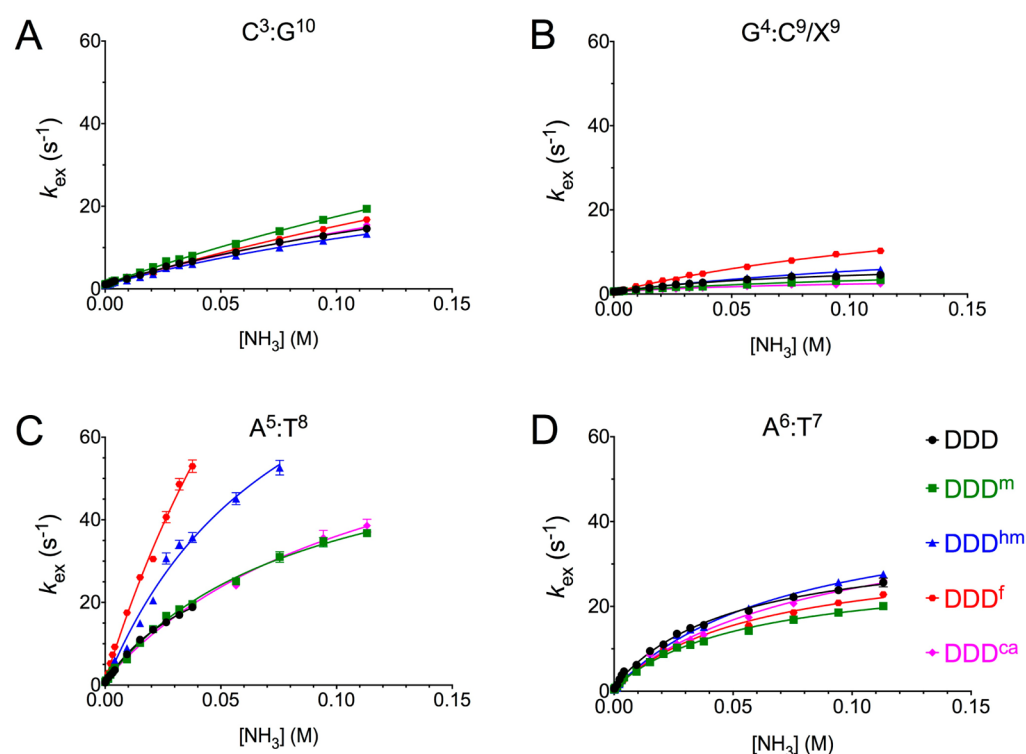


Figure 2. Plots showing imino proton exchange rates obtained by monitoring magnetization from water as a function of ammonia base catalyst: (A) base pair C³:G¹⁰, (B) base pair G⁴:C⁹, (C) base pair A⁵:T⁸, and (D) base pair A⁶:T⁷ in the DDD (black), DDD^m (green), DDD^{hm} (blue), DDD^f (red), and DDD^{ca} (pink) duplexes.

Table 2. Rate and Equilibrium Constants for DNA Base Pair Opening

	k_0 (s ⁻¹) ^a				
	DDD	DDD ^m	DDD ^{hm}	DDD ^f	DDD ^{ca}
C ³ :G ¹⁰	1.1 ± 0.06	1.0 ± 0.07	0.95 ± 0.05	0.71 ± 0.03	1.1 ± 0.06
G ⁴ :C ⁹	0.57 ± 0.03	0.56 ± 0.1	0.68 ± 0.05	0.39 ± 0.04	0.49 ± 0.04
A ⁵ :T ⁸	0.59 ± 0.03	0.73 ± 0.07	0.77 ± 0.03	0.79 ± 0.04	0.59 ± 0.03
A ⁶ :T ⁷	0.61 ± 0.03	0.43 ± 0.04	0.36 ± 0.01	0.27 ± 0.03	0.55 ± 0.03
	k_{op} (s ⁻¹)				
	DDD	DDD ^m	DDD ^{hm}	DDD ^f	DDD ^{ca}
C ³ :G ¹⁰	45 ± 3	90 ± 12	42 ± 5	86 ± 18	64 ± 12
G ⁴ :C ⁹	8 ± 0.5	7 ± 0.6	16 ± 2	26 ± 2	4 ± 0.3
A ⁵ :T ⁸	40 ± 2	65 ± 2	110 ± 13	222 ± 53	58 ± 5
A ⁶ :T ⁷	36 ± 1	29 ± 1	45 ± 2	33 ± 3	44 ± 3
	k_{cl} (×10 ⁻⁷ s ⁻¹)				
	DDD	DDD ^m	DDD ^{hm}	DDD ^f	DDD ^{ca}
C ³ :G ¹⁰	15 ± 1	25 ± 2	17 ± 1	21 ± 2	20 ± 1
G ⁴ :C ⁹	6.7 ± 0.2	9.4 ± 1	13 ± 0.8	9.3 ± 1	6.6 ± 0.1
A ⁵ :T ⁸	0.97 ± 0.04	1.9 ± 0.04	1.5 ± 0.05	2.1 ± 0.06	2.3 ± 0.05
A ⁶ :T ⁷	0.98 ± 0.09	1.1 ± 0.08	1.6 ± 0.08	1.1 ± 0.05	1.3 ± 0.01
	$K_{op} \times 10^7$				
	DDD	DDD ^m	DDD ^{hm}	DDD ^f	DDD ^{ca}
C ³ :G ¹⁰	2.9 ± 0.1	3.6 ± 0.1	2.5 ± 0.1	3.8 ± 0.1	3.2 ± 0.08
G ⁴ :C ⁹	1.2 ± 0.04	0.75 ± 0.04	1.2 ± 0.06	2.8 ± 0.1	0.6 ± 0.04
A ⁵ :T ⁸	41 ± 0.08	35 ± 2	73 ± 6	106 ± 4	34 ± 1
A ⁶ :T ⁷	37 ± 5	26 ± 3	29 ± 3	29 ± 2	34 ± 0.9

^aThe observed exchange rate without an ammonia catalyst.

acceptors is sufficient for rapid exchange from the open state ($k_{ex,open} \gg k_{cl}$), so exchange occurs at each opening event and $k_{ex} = k_{op}$. In the EX2 regime, where the concentration of base is low ($k_{ex,open} \ll k_{cl}$), the rate of exchange from the open state is

proportional to the exchange rate and the concentration of the acceptor.^{75–77}

Figure 2 shows the results for the C³:G¹⁰, G⁴:C⁹, A⁵:T⁸, and A⁶:T⁷ base pairs of the DDD^{hm}, DDD^f, and DDD^{ca} duplexes.

They were compared to both the unmodified DDD and to the DDD^m duplexes. Plots of exchange rates as a function of ammonia concentration suggested that the EX1 regime^{75–77} was attained. Consistent with the results of Moe et al.,⁴⁵ the rates of imino proton exchange were lower for G:C base pairs C³:G¹⁰ and G⁴:X⁹ and greater for A:T base pairs A⁵:T⁸ and A⁶:T⁷. At 15 °C, the oxidized cytosines differentially altered exchange rates of the imino protons of the C³:G¹⁰, G⁴:X⁹, A⁵:T⁸, and A⁶:T⁷ base pairs. The greatest effects were observed at the neighbor A⁵:T⁸ base pair. For the DDD^{hm} and DDD^f duplexes, the exchange rate of the A⁵:T⁸ base pair imino proton increased at all concentrations of ammonia (Figure 2). There was a 3-fold increased rate of base pair opening in the DDD^{hm} duplex and a 5-fold increased rate of base pair opening in the DDD^f duplex, with respect to the DDD duplex (Table 2). In contrast, for the DDD^{ca} duplex, the exchange rate of the A⁵:T⁸ imino proton was similar to those of the DDD and DDD^m duplexes at all concentrations of ammonia. These differences were reflected in measurements of the respective equilibrium constants for base pair opening. For the DDD^{hm} duplex, the equilibrium constant for base pair opening (αK_{op}) at base pair A⁵:T⁸ was 7.3×10^8 , and for the DDD^f duplex, the equilibrium constant for base pair opening at A⁵:T⁸ was 1.1×10^9 , differing from the DDD and DDD^m duplexes (3.4×10^8 and 3.5×10^8 , respectively). In contrast, for the DDD^{ca} duplex, the equilibrium constant for base pair opening of A⁵:T⁸ was 4.1×10^8 , similar to that of the DDD and DDD^m duplexes. The neighbor effect did not extend beyond the A⁵:T⁸ base pair. At base pair A⁶:T⁷, exchange rates as a function of ammonia concentration were comparable for all duplexes.

A smaller effect on base pair opening dynamics was observed at the G⁴:X⁹ base pair. For the DDD^f duplex, the exchange rate of G⁴:X⁹ was greater at all concentrations of ammonia than that for the DDD^{hm}, DDD^{ca}, DDD^m, and DDD duplexes ($k_{op} = 26 \text{ s}^{-1}$ in DDD^f vs $k_{op} = 16, 4, 7,$ and 8 s^{-1} for DDD^{hm}, DDD^{ca}, DDD^m, and DDD, respectively). For the DDD^f duplex, the equilibrium constant for base pair opening increased 3-fold, calculated as 2.8×10^7 vs $1.2 \times 10^7, 7.5 \times 10^6, 1.2 \times 10^7,$ and 6.0×10^6 , respectively, for the DDD, DDD^m, DDD^{hm}, and DDD^{ca} duplexes.

In contrast, base pair opening dynamics at the neighboring C³:G¹⁰ base pair were not affected by the presence of the oxidized cytosines in the DDD^{hm}, DDD^f, or DDD^{ca} duplex. Thus, the differences in base pair opening dynamics for the 5hmC, 5fC, and 5caC bases in the 5'-T⁸X⁹G¹⁰-3' sequence of the DDD exhibit a pronounced sequence dependence, with the greatest effects being evident at the neighboring A⁵:T⁸ base pair. This is the base pair located in the 5'-direction with respect to the oxidized cytosine X⁹. The overall results are summarized in Table 2.

Structures of the DDD^{hm}, DDD^f, and DDD^{ca} Duplexes.

The modified DDD^{hm}, DDD^f, and DDD^{ca} duplexes yielded diffraction-quality crystals. Crystals belonged to the orthorhombic P2₁2₁2₁ space group. The crystal structures were determined using the unmodified DDD (PDB ID code 436D)⁴⁰ as a search model for molecular replacement. Structures were refined using anisotropic B factors to a resolution of 1.02 Å for DDD^{hm} and isotropic B factors to resolutions of 1.90 and 1.95 Å for DDD^f and DDD^{ca}, respectively. Each of the structures was compared to that of the DDD.⁴⁰ Overall, the structures were similar to the DDD,⁴⁰ as indicated by comparative rmsd analyses, with rmsd values of 0.67, 0.46, and 0.49 Å for DDD^{hm}, DDD^f, and DDD^{ca},

respectively. Classical features of the DDD, including waters forming the minor groove spine of hydration,⁷⁸ were conserved. The data and refinement statistics are provided in Table 1.

Figure 3 shows electron density and base pairing arrangements for the 5hmC:G, 5fC:G, and 5caC:G base pairs in the

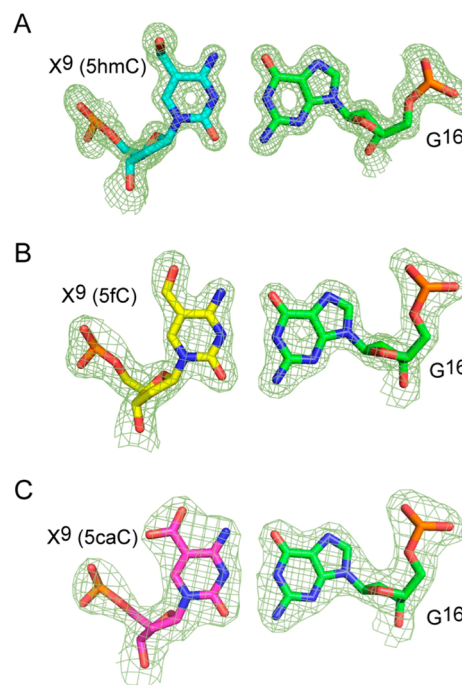


Figure 3. Fourier ($2F_o - F_c$) sum electron density contoured at the 1.0σ level (green meshwork) around the (A) 5hmC:G, (B) 5fC:G, and (C) 5caC:G base pairs showing Watson–Crick base pairing geometry.

DDD^{hm}, DDD^f, and DDD^{ca} duplexes, respectively. Watson–Crick base pairing was evident, and the hydroxymethyl, formyl, or carboxyl moieties of the oxidized cytosines were oriented into the major groove. The formyl group of 5fC and the carboxyl group of 5caC were within hydrogen-bonding range of the N⁴ exocyclic amines of the oxidized cytosines. For the DDD^{hm} duplex, electron density associated with the hydroxymethyl moiety of 5hmC suggested partial occupancy of two conformations. The major conformation refined with occupancy 0.8, and the minor conformation refined with occupancy 0.2. In the major conformation, the hydroxyl group hydrogen bonded with the terminal N1 ammonium moiety of a spermine and with G¹⁰ O⁶ via an ordered water molecule (Figure S2 of the Supporting Information). In the minor conformation, the hydroxyl group was oriented toward the backbone phosphate and formed interactions with neighboring waters (Figure S3 of the Supporting Information). A hydrogen bond was also observed between the hydroxyl group at the modified cytosine X²¹ and an axially coordinated water (HOH 12) at a distance of 2.7 Å, with a further interaction to G²² N7 (2.8 Å). An additional hydrogen bond was observed between the X²¹ hydroxyl and G²² O⁶ via water HOH 11 (3.0 Å distance from X²¹ to HOH 11 and 2.7 Å from HOH 11 to G²² O⁶) (Figures S2 and S3 of the Supporting Information). Base stacking patterns for the DDD^{hm}, DDD^f, and DDD^{ca} duplexes were similar (Figure 4).

The DDD^{hm}, DDD^f, and DDD^{ca} duplexes were also examined by NMR,^{44,46,47} using standard methods.^{79,80} The sequential base aromatic → deoxyribose anomeric NOEs were

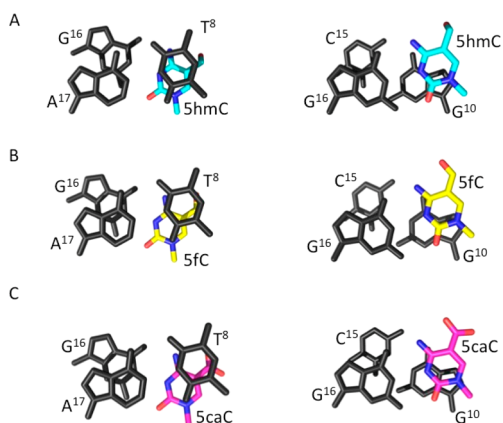


Figure 4. (A) DDD^{hm} , (B) DDD^f , and (C) DDD^{ca} structures, illustrating stacking interactions at oxidation sites.

identified from $C^1 \rightarrow G^{12}$ (Figure S4 of the Supporting Information). For the DDD^{hm} , DDD^f , and DDD^{ca} duplexes (and as well for the DDD and DDD^m duplexes), the intensities of NOE cross-peaks between the purine H8 and pyrimidine H6 protons and the deoxyribose H1' protons were of the same relative magnitudes as those between other bases in the sequence, indicating that the glycosyl bonds maintained the anti conformations. In all instances, the NOE connectivity of the purine N1H and pyrimidine N3H protons⁷⁴ was obtained from $G^2:C^{11} \rightarrow C^3:G^{10} \rightarrow G^4:X^9 \rightarrow A^5:T^8 \rightarrow A^6:T^7$ (Figure 5). NOE cross-peaks from the oxidized base $X^9 N^4H1$ and N^4H2 protons to the complementary base $G^4 N1H$ proton were observed, as well as interactions to neighbor bases $T^8 N3H$ and $G^{10} N1H$, consistent with Watson–Crick geometry being favored,

corroborating the crystallographic data (Figure 3). Significantly, evidence for intranucleotide hydrogen bonding involving the formyl group of 5fC or the carboxyl group of 5caC and the N^4 exocyclic amine of 5fC or 5caC was evident in NMR spectra of the DDD^f and DDD^{ca} duplexes, for which both of the $X^9 N^4$ amino proton resonances shift downfield into the 7.8–8.8 ppm spectral range (Figure 5). The effect was most pronounced for the DDD^{ca} duplex. In contrast, for the DDD , DDD^m , and DDD^{hm} duplexes, one of the N^4 amino protons shifts downfield, consistent with the maintenance of a Watson–Crick base pair, whereas the other remains in the 6.5–7.0 ppm spectral range, which is the anticipated result given that cytosine, 5mC, and 5hmC cannot form this hydrogen bond. Overall, the NMR data corroborated the crystallographic data, giving no indication of the presence of imino tautomers and suggesting that each of the oxidized cytosines participated in normal Watson–Crick base pairing when placed opposite guanine.

DISCUSSION

The 5hmC,^{10,26,27} 5fC,²⁷ and 5caC^{27,29,30} oxidation products of 5mC are intermediates in active demethylation^{8–25} and have potential roles in epigenetic regulation of cellular function.^{6,7} Their removal is orchestrated by glycosylase-mediated base excision repair; TDG is essential for active DNA demethylation.⁸ It has been reported that 5fC and 5caC, but not 5hmC, are substrates for thymine DNA glycosylase (TDG).¹⁴ Accordingly, it was of interest to determine whether these oxidized cytosines differentially alter duplex DNA and how such differences correlate with differences in excision of 5hmC, 5fC, and 5caC by TDG.¹⁴ The Dickerson–Drew dodecamer (DDD)^{38,39} provided a platform for conducting these studies. It

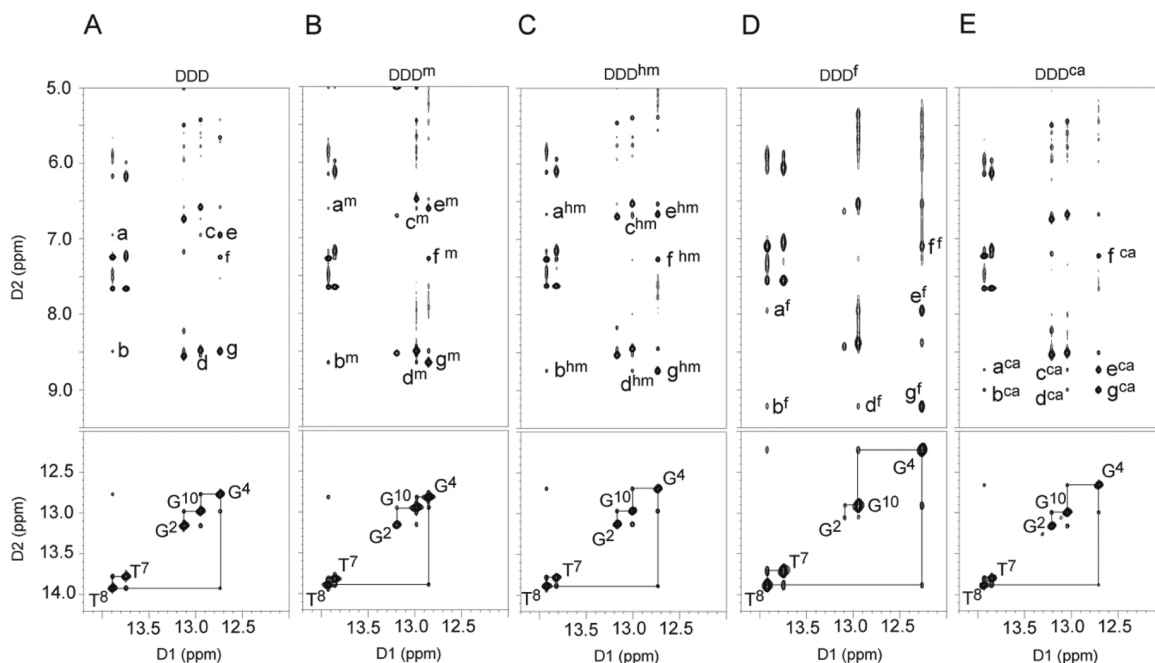


Figure 5. NOESY spectra depicting resonances for the thymine and guanine imino protons and sequential NOE connectivity for the imino protons of the base pairs $G^2:C^{11}$ to $A^6:T^7$ for (A) DDD , (B) DDD^m , (C) DDD^{hm} , (D) DDD^f , and (E) DDD^{ca} duplexes (lower panels). Expansion of the NOESY spectra for (A) DDD , (B) DDD^m , (C) DDD^{hm} , (D) DDD^f , and (E) DDD^{ca} duplexes (upper panels), illustrating the conservation of Watson–Crick base pairing and base stacking at the modification sites: a, C^9 or $X^9 N^4H1 \rightarrow T^8 N3H$; b, C^9 or $X^9 N^4H2 \rightarrow T^8 N3H$; c, C^9 or $X^9 N^4H1 \rightarrow G^{10} N1H$; d, C^9 or $X^9 N^4H2 \rightarrow G^{10} N1H$; e, C^9 or $X^9 N^4H1 \rightarrow G^4 N1H$; f, $A^5 H2 \rightarrow G^4 N1H$; and g, C^9 or $X^9 N^4H2 \rightarrow G^4 N1H$. (Indices m, hm, f, or ca refer to the base pairs in the modified duplexes, DDD^m , DDD^{hm} , DDD^f , and DDD^{ca} , respectively.) Data were collected at 900 MHz.

contains the 5'-CG-3' sequence associated with genomic cytosine methylation, and, most importantly, it is simultaneously amenable to crystallographic^{38–43} and spectroscopic^{44–47} analyses.

Stabilization of the DDD by 5caC. The presence of 5caC in the 5'-T⁸X⁹G¹⁰-3' sequence stabilizes the DDD, as evidenced by the 6–8 °C increase in T_m for the DDD^{ca} as compared to the T_m values of the DDD and of the DDD^m under the same conditions. NMR data for the base paired guanine N1H and thymine N3H imino protons (Figure 1) confirm this conclusion. For the DDD^{ca} duplex, at temperatures as high as 55 °C, the imino proton resonances of base pairs C³:G¹⁰, G⁴:X⁹, and A⁵:T⁸ remain detectable (Figure 1E). In contrast, for the DDD^{hm} duplex and DDD^f duplexes, the imino proton resonances of base pairs C³:G¹⁰, G⁴:X⁹, and A⁵:T⁸ broaden at temperatures above 35 °C (Figure 1C,D). While the inclusion of 5caC into the 5'-T⁸X⁹G¹⁰-3' sequence in the DDD provides only a single data point for thermodynamic comparison, the observation that 5caC stabilizes the DDD^{ca} is consistent with calculations performed by Sumino et al.⁸¹ It also corroborates data obtained by the same group for the stabilities of 13-mers and 14-mers containing 5caC. This stabilization of the DDD^{ca} is not attributable to improved base stacking geometry of 5caC in DDD^{ca} because 5caC exhibits a base stacking geometry in the DDD that is similar to both 5hmC and 5fC (Figure 4). However, electronic dipole–dipole interactions associated with 5caC^{14,23} might enhance the thermodynamic stability of the DDD^{ca} duplex without disturbing the stacking geometry.

Sequence-Specific Base Pair Opening Dynamics of the Oxidized Duplexes. The imino proton exchange rates at base pairs C³:G¹⁰, G⁴:X⁹, and A⁵:T⁸ depend upon the identity of the cytosine oxidation product and exhibit sequence dependence. The greatest effects are observed for the neighbor base pair A⁵:T⁸, with a smaller effect at G⁴:X⁹ and minimal effect at the neighbor base pair C³:G¹⁰. Base pair A⁵:T⁸ is the 5'-neighbor with respect to the oxidized cytosine at position X⁹, whereas base pair C³:G¹⁰ is the 3'-neighbor with respect to the oxidized cytosine at position X⁹ (Chart 1). While the A⁵:T⁸ base pair of the DDD intrinsically exhibits enhanced exchange kinetics,⁴⁵ the presence of either 5fC or 5hmC further enhances imino proton exchange rates at A⁵:T⁸, whereas the presence of 5caC does not (Figure 2), an observation that is consistent with the thermal stabilization of the duplex by 5caC as opposed to 5fC or 5hmC. Thus, for DDD^f, base pair A⁵:T⁸ base pair opens with the frequency of $k_{op} = 222 \text{ s}^{-1}$, five times faster than in the DDD. For the DDD^{hm} duplex, base pair A⁵:T⁸ opens three times faster than in the DDD ($k_{op} = 110 \text{ s}^{-1}$ vs $k_{op} = 40 \text{ s}^{-1}$ in DDD^{hm} and DDD, respectively).

Structures of Duplexes Containing 5hmC, 5fC, or 5caC. Evidence for wobble base pairing geometry at oxidized cytosines,^{17,19,23,36,37} arising from imino tautomers of 5caC or 5fC,^{20,37} is not observed. The results are consistent with calculations of the stabilities of the amino and imino tautomers of 5fC and 5caC at the nucleobase level, which have suggested that, when paired with G, both 5fC and 5caC preferentially form Watson–Crick pairs.²³ Instead, each of the 5hmC, 5fC, and 5caC oxidation products favors Watson–Crick hydrogen-bonding interactions when located in the 5'-T⁸X⁹G¹⁰-3' sequence (Figures 3–5).

A common structural feature of 5fC and 5caC in the DDD is formation of intranucleobase hydrogen bonds between the carbonyl oxygens of the formyl or carboxyl groups, respectively, and a cytosine N⁴H amino proton. This hydrogen bond had

been observed between the exocyclic N⁴ amino group and the formyl oxygen at C5 of 5fC at the nucleoside level.^{27,82} The downfield shifts of both of the X⁹ N⁴ amino proton resonances into the 7.8–8.8 ppm spectral range is evident in NMR spectra of the DDD^f and DDD^{ca} duplexes (Figure 5) and is consistent with the formation of these hydrogen bonds. The NMR data corroborates the crystallographic structure data (Figure 3), which shows that the carbonyl oxygens of the formyl or carboxyl groups of 5fC or 5caC, respectively, and a cytosine N⁴H amino proton are within hydrogen-bonding distance. The effect in the NMR data is most pronounced for the DDD^{ca} duplex (Figure 5). In the crystallographic structure of the DDD^{ca} duplex (Figure 3), this hydrogen bond keeps the carboxyl group in plane with the oxidized cytosine. For the DDD, DDD^m, and DDD^{hm} duplexes, one of the N⁴ amino protons shifts downfield, consistent with the maintenance of a Watson–Crick base pair, whereas the other remains in the 6.5–7.0 ppm spectral range, which is the anticipated result given that cytosine, 5mC, and 5hmC cannot form this hydrogen bond.

Structure–Activity Relationships. DNA glycosylases³⁶ typically employ an extrahelical base-flipping mechanism^{35,83–89} to position substrates for catalysis. Differences in the ability of TDG to excise 5fC, 5caC, or 5hmC from DNA¹⁴ could be mediated by differential recognition of these oxidized cytosine bases in DNA. Stivers et al.^{61,90–93} demonstrated that damage recognition by a different glycosylase, uracil DNA glycosylase (UDG), is facilitated by enhanced base pair opening rates for destabilized A:U base pairs.³⁵ The present data reveal that site- and sequence-specific differences with regard to duplex stability and base pair opening dynamics are observed when the 5hmC, 5fC, and 5caC are placed into the DDD^{hm}, DDD^f, and DDD^{ca} dodecamers within the 5'-T⁸X⁹G¹⁰-3' sequence. Neither the stabilization of the DDD by 5caC nor the differences in base pair opening dynamics correlate with differences in the excision of 5hmC, 5fC, and 5caC by TDG, as reported by Maiti et al.¹⁴ Both 5hmC and 5fC exhibit increased base pair opening rates at the neighboring A⁵:T⁸ base pair. However, only 5fC is excised by TDG. Moreover, 5caC, which also is excised by TDG, thermally stabilizes the DDD^{ca} and does not exhibit increased base pair opening kinetics at the 5'-neighbor A⁵:T⁸ base pair (Figure 2).

It has been proposed that the imino tautomers of 5caC or 5fC adopt wobble-like base pairing geometry with the complementary G, which might provide a basis for recognition by TDG.^{20,37} The present crystallographic and NMR data indicate that the 5hmC, 5fC, and 5caC bases each favor Watson–Crick base pairing in the DDD duplex. This argues against wobble base pairing involving imino tautomers of these oxidized cytosines as a primary mode of recognition by TDG. However, the presence of small amounts of the imino tautomers cannot be ruled out, nor can a shift from Watson–Crick base pairing to wobble pairing subsequent to enzyme binding. It has been proposed that the hydrogen bond between the exocyclic N⁴ amine and the formyl or carboxyl oxygen at C5 of the 5fC or the 5caC base might shift the equilibrium toward the imino tautomer^{94,95} and lead to protonation at N3 of the oxidized cytosine.^{37,96} Additionally, other factors such as electrostatic and steric contributions, which remain to be examined, might modulate the differential recognition of these oxidized cytosines by TDG.

Alternatively, differences in the ability of TDG to excise 5fC, 5caC, or 5hmC from DNA could be controlled by differences

in the catalytic step of base excision, once the oxidized cytosine bases have been inserted into the active site of the glycosylase. Maiti et al.⁹⁷ implied a role of the conserved Asn¹⁴⁰ in the chemical step and of the conserved Arg²⁷⁵ in nucleotide flipping into the active site. In additional studies, Maiti et al.¹⁴ accounted for the differential excision ability of TDG with respect to 5hmC, 5fC, and ScaC by arguing that activity is greatest for oxidized cytosines possessing electron-withdrawing substituents at the C5 carbon, which stabilize developing negative charge in the transition state complex for base excision. Following their argument, 5fC is a good substrate and 5hmC is not.¹⁴ At neutral pH, ScaC exists as an anion with pK_a values of 2.4 for the carboxyl and 4.3 for the N3 position,²³ and catalysis is facilitated because the ionized carboxyl group lowers the pK_a of cytosine and stabilization of the carboxyl by the exocyclic amine of cytosine creates an electron-withdrawing effect.^{14,23} Maiti et al.²³ demonstrated that the excision ability of TDG with respect to 5fC is pH-independent but that the excision of ScaC is acid-catalyzed. Moreover, Zhang et al.²⁵ found that TDG binds to ScaC with greater affinity than to 5fC, U, or T and proposed that residues Asn¹⁵⁷, His¹⁵¹, and Tyr¹⁵² are involved in hydrogen bonds with the ScaC carboxyl group. Finally, the structure of TDG in complex with DNA containing a G:5hmU mismatch showed that TDG engages in hydrogen-bonding interactions with both 5hmU and ScaC.¹⁹

The present results are consistent with the proposal by Maiti et al.,¹⁴ in which the excision specificity of TDG for 5fC and ScaC vs 5hmC is dictated by differences in the enzyme–substrate complex transition state. Both 5fC and ScaC form hydrogen bonds between the carbonyl oxygens of their formyl or carboxyl groups, respectively, and a cytosine exocyclic N⁴H amino proton. The electron-withdrawing effect of the 5fC and ScaC substituents^{14,23} should be enhanced by hydrogen bonding between the carbonyl oxygens of their formyl or carboxyl groups, respectively, and a cytosine exocyclic N⁴H amino proton. This would be anticipated to stabilize developing negative charge in the transition state complex for base excision.

Summary. The cytosine oxidation products 5hmC, 5fC, and ScaC exhibit differences in thermodynamics and base pair opening dynamics when placed into the 5'-T⁸X⁹G¹⁰-3' sequence of the DDD, but these do not correlate with differences in the ability of TDG to excise these cytosine oxidation products.¹⁴ While TDG may exploit thermodynamic and base pair opening dynamics in the recognition of oxidized cytosines in DNA, differences in the transition state complexes for the base excision step may be rate-limiting with respect to the chemical step of base excision. Of course, the 5'-T⁸X⁹G¹⁰-3' sequence is just one sequence, and it will be of interest to further examine the sequence dependence of these effects, particularly in light of the recent report from Raiber et al.³⁴ showing that the presence of three 5fC sites in an iterated CG repeat sequence changes the geometry of the DNA grooves and base pairs containing the 5fC oxidation product. DNA glycosylases may exploit different mechanistic pathways toward base excision. The recognition of uracil by uracil DNA glycosylase (UDG) is reported to be facilitated by enhanced base pair opening rates at A:U base pairs.³⁵ Interestingly, the 5mC DNA glycosylase DEMETER (DME) removes 5mC, 5hmC, and ScaC but has no activity for 5fC.^{99,98} Its inactivity toward 5fC also does not seem to be correlated with 5fC base pair opening rates, and it does not seem to correlate with the electron-withdrawing effect of the 5fC and ScaC substituents.^{14,23}

■ ASSOCIATED CONTENT

📄 Supporting Information

Tables S1: Crystallization conditions for the DDD^{hm}, DDD^f, and DDD^{ca} duplexes. Figure S1: Temperature dependence of line widths of the imino proton resonances of the DDD, DDD^m, DDD^{hm}, DDD^f, and DDD^{ca} duplexes. Figure S2: Modification site of the DDD^{hm} duplex displaying interactions between the modified 5hmC and 3'-flanking G²² through water molecules. Figure S3: Modification site of the DDD^{hm} duplex displaying interactions between the modified 5hmC and 3'-flanking G²² through water molecules. Figure S4: Expanded plots from NOESY spectra, depicting sequential NOE connectivities of the DDD, DDD^m, DDD^{hm}, DDD^f, and DDD^{ca} duplexes. This material is available free of charge via the Internet at <http://pubs.acs.org>.

■ AUTHOR INFORMATION

Corresponding Author

*(M.P.S.) Tel.: 615-322-2589; E-mail: michael.p.stone@vanderbilt.edu

Funding

This work was supported by NIH grants R01 CA-55678 (M.P.S.), R01 ES-019625 (B.F.E.), and P41 GM103403 (NE-CAT). Funding for NMR was supplied by NIH grants S10 RR-05805 and S10 RR-025677 and NSF grant DBI 0922862, the latter was funded by the American Recovery and Reinvestment Act of 2009 (Public Law 111-5). Vanderbilt University assisted with the purchase of NMR instrumentation. Use of the Advanced Photon Source was supported by the U.S. Department of Energy, Office of Science, Office of Basic Energy Sciences, under contract no. DE-AC02-06CH11357.

Notes

The authors declare no competing financial interest.

■ ACKNOWLEDGMENTS

We thank Edward Hawkins (deceased), Dr. Plamen Christov, and Professor Carmelo J. Rizzo for help and guidance with synthesis of oligodeoxynucleotides.

■ ABBREVIATIONS

ScaC, 5-carboxylcytosine; 5fC, 5-formylcytosine; 5hmC, 5-hydroxymethylcytosine; 5mC, 5-methylcytosine; DDD, Dickerson–Drew dodecamer; DME, DNA glycosylase DEMETER; DSS, 4,4-dimethyl-4-silapentane-1-sulfonic acid; EDTA, ethylenediaminetetraacetic acid, sodium salt; MPD, 2-methyl-2,4-pentandiol; NOE, nuclear Overhauser effect; NOESY, two-dimensional nuclear Overhauser enhancement spectroscopy; TDG, thymine DNA glycosylase; TET, ten-eleven translocation dioxygenase; UDG, uracil DNA glycosylase

■ REFERENCES

- (1) Bestor, T. H. (1988) Cloning of a mammalian DNA methyltransferase. *Gene* 74, 9–12.
- (2) Bestor, T., Laudano, A., Mattaliano, R., and Ingram, V. (1988) Cloning and sequencing of a cDNA encoding DNA methyltransferase of mouse cells. The carboxyl-terminal domain of the mammalian enzymes is related to bacterial restriction methyltransferases. *J. Mol. Biol.* 203, 971–983.
- (3) Pfeifer, G. P., Steigerwald, S. D., and Grunwald, S. (1989) The DNA methylation system in proliferating and differentiated cells. *Cell Biophys.* 15, 79–86.

- (4) Okano, M., Bell, D. W., Haber, D. A., and Li, E. (1999) DNA methyltransferases Dnmt3a and Dnmt3b are essential for *de novo* methylation and mammalian development. *Cell* 99, 247–257.
- (5) Wyatt, G. R. (1950) Occurrence of 5-methylcytosine in nucleic acids. *Nature* 166, 237–238.
- (6) Meissner, A. (2010) Epigenetic modifications in pluripotent and differentiated cells. *Nat. Biotechnol.* 28, 1079–1088.
- (7) Feng, S., Jacobsen, S. E., and Reik, W. (2010) Epigenetic reprogramming in plant and animal development. *Science* 330, 622–627.
- (8) Wu, S. C., and Zhang, Y. (2010) Active DNA demethylation: many roads lead to Rome. *Nat. Rev. Mol. Cell Biol.* 11, 607–620.
- (9) Globisch, D., Munzel, M., Muller, M., Michalakakis, S., Wagner, M., Koch, S., Bruckl, T., Biel, M., and Carell, T. (2010) Tissue distribution of 5-hydroxymethylcytosine and search for active demethylation intermediates. *PLoS One* 5, e15367.
- (10) Munzel, M., Globisch, D., and Carell, T. (2011) 5-Hydroxymethylcytosine, the sixth base of the genome. *Angew. Chem., Int. Ed.* 50, 6460–6468.
- (11) Gu, T. P., Guo, F., Yang, H., Wu, H. P., Xu, G. F., Liu, W., Xie, Z. G., Shi, L., He, X., Jin, S. G., Iqbal, K., Shi, Y. G., Deng, Z., Szabo, P. E., Pfeifer, G. P., Li, J., and Xu, G. L. (2011) The role of Tet3 DNA dioxygenase in epigenetic reprogramming by oocytes. *Nature* 477, 606–610.
- (12) Iqbal, K., Jin, S. G., Pfeifer, G. P., and Szabo, P. E. (2011) Reprogramming of the paternal genome upon fertilization involves genome-wide oxidation of 5-methylcytosine. *Proc. Natl. Acad. Sci. U.S.A.* 108, 3642–3647.
- (13) Wossidlo, M., Nakamura, T., Lepikhov, K., Marques, C. J., Zakhartchenko, V., Boiani, M., Arand, J., Nakano, T., Reik, W., and Walter, J. (2011) 5-Hydroxymethylcytosine in the mammalian zygote is linked with epigenetic reprogramming. *Nat. Commun.* 2, 241.
- (14) Maiti, A., and Drohat, A. C. (2011) Thymine DNA glycosylase can rapidly excise 5-formylcytosine and 5-carboxylcytosine: Potential implications for active demethylation of CpG sites. *J. Biol. Chem.* 286, 35334–35338.
- (15) He, Y. F., Li, B. Z., Li, Z., Liu, P., Wang, Y., Tang, Q., Ding, J., Jia, Y., Chen, Z., Li, L., Sun, Y., Li, X., Dai, Q., Song, C. X., Zhang, K., He, C., and Xu, G. L. (2011) Tet-mediated formation of 5-carboxylcytosine and its excision by TDG in mammalian DNA. *Science* 333, 1303–1307.
- (16) Maiti, A., and Drohat, A. C. (2011) Dependence of substrate binding and catalysis on pH, ionic strength, and temperature for thymine DNA glycosylase: insights into recognition and processing of G·T mismatches. *DNA Repair* 10, 545–553.
- (17) Cortellino, S., Xu, J., Sannai, M., Moore, R., Caretti, E., Cigliano, A., Le Coz, M., Devarajan, K., Wessels, A., Soprano, D., Abramowitz, L. K., Bartolomei, M. S., Rambow, F., Bassi, M. R., Bruno, T., Fanciulli, M., Renner, C., Klein-Szanto, A. J., Matsumoto, Y., Kobi, D., Davidson, I., Alberti, C., Larue, L., and Bellacosa, A. (2011) Active DNA demethylation by thymine DNA glycosylase. *Environ. Mol. Mutagen.* 52, S14–S14.
- (18) Cortellino, S., Xu, J. F., Sannai, M., Moore, R., Caretti, E., Cigliano, A., Le Coz, M., Devarajan, K., Wessels, A., Soprano, D., Abramowitz, L. K., Bartolomei, M. S., Rambow, F., Bassi, M. R., Bruno, T., Fanciulli, M., Renner, C., Klein-Szanto, A. J., Matsumoto, Y., Kobi, D., Davidson, I., Alberti, C., Larue, L., and Bellacosa, A. (2011) Thymine DNA glycosylase is essential for active DNA demethylation by linked deamination-base excision repair. *Cell* 146, 67–79.
- (19) Hashimoto, H., Hong, S., Bhagwat, A. S., Zhang, X., and Cheng, X. (2012) Excision of 5-hydroxymethyluracil and 5-carboxylcytosine by the thymine DNA glycosylase domain: its structural basis and implications for active DNA demethylation. *Nucleic Acids Res.* 40, 10203–10214.
- (20) Hashimoto, H., Zhang, X., and Cheng, X. (2012) Excision of thymine and 5-hydroxymethyluracil by the MBD4 DNA glycosylase domain: structural basis and implications for active DNA demethylation. *Nucleic Acids Res.* 40, 8276–8284.
- (21) Maiti, A., Noon, M. S., MacKerell, A. D., Jr., Pozharski, E., and Drohat, A. C. (2012) Lesion processing by a repair enzyme is severely curtailed by residues needed to prevent aberrant activity on undamaged DNA. *Proc. Natl. Acad. Sci. U.S.A.* 109, 8091–8096.
- (22) Cadet, J., and Wagner, J. R. (2014) TET enzymatic oxidation of 5-methylcytosine, 5-hydroxymethylcytosine and 5-formylcytosine. *Mutat. Res., Genet. Toxicol. Environ. Mutagen.* 764–765, 18–35.
- (23) Maiti, A., Michelson, A. Z., Armwood, C. J., Lee, J. K., and Drohat, A. C. (2013) Divergent mechanisms for enzymatic excision of 5-formylcytosine and 5-carboxylcytosine from DNA. *J. Am. Chem. Soc.* 135, 15813–15822.
- (24) Wossidlo, M., Arand, J., Sebastiano, V., Lepikhov, K., Boiani, M., Reinhardt, R., Scholer, H., and Walter, J. (2010) Dynamic link of DNA demethylation, DNA strand breaks and repair in mouse zygotes. *EMBO J.* 29, 1877–1888.
- (25) Zhang, P., Su, L., Wang, Z., Zhang, S., Guan, J., Chen, Y., Yin, Y., Gao, F., Tang, B., and Li, Z. (2012) The involvement of 5-hydroxymethylcytosine in active DNA demethylation in mice. *Biol. Reprod.* 86, 104.
- (26) Kriaucionis, S., and Heintz, N. (2009) The nuclear DNA base 5-hydroxymethylcytosine is present in Purkinje neurons and the brain. *Science* 324, 929–930.
- (27) Munzel, M., Lischke, U., Stathis, D., Pfaffeneder, T., Gnerlich, F. A., Deiml, C. A., Koch, S. C., Karaghiosoff, K., and Carell, T. (2011) Improved synthesis and mutagenicity of oligonucleotides containing 5-hydroxymethylcytosine, 5-formylcytosine and 5-carboxylcytosine. *Chemistry* 17, 13782–13788.
- (28) Simmons, J. M., Muller, T. A., and Hausinger, R. P. (2008) Fe(II)/alpha-ketoglutarate hydroxylases involved in nucleobase, nucleoside, nucleotide, and chromatin metabolism. *Dalton Trans.* 5132–5142.
- (29) Tahiliani, M., Koh, K. P., Shen, Y., Pastor, W. A., Bandukwala, H., Brudno, Y., Agarwal, S., Iyer, L. M., Liu, D. R., Aravind, L., and Rao, A. (2009) Conversion of 5-methylcytosine to 5-hydroxymethylcytosine in mammalian DNA by MLL partner TET1. *Science* 324, 930–935.
- (30) Ito, S., D'Alessio, A. C., Taranova, O. V., Hong, K., Sowers, L. C., and Zhang, Y. (2010) Role of Tet proteins in 5mC to 5hmC conversion, ES-cell self-renewal and inner cell mass specification. *Nature* 466, 1129–1133.
- (31) Bienvenu, C., Wagner, J. R., and Cadet, J. (1996) Photosensitized oxidation of 5-methyl-2'-deoxycytidine by 2-methyl-1,4-naphthoquinone: characterization of 5-(hydroperoxymethyl)-2'-deoxycytidine and stable methyl group oxidation products. *J. Am. Chem. Soc.* 118, 11406–11411.
- (32) Ito, S., Shen, L., Dai, Q., Wu, S. C., Collins, L. B., Swenberg, J. A., He, C., and Zhang, Y. (2011) Tet proteins can convert 5-methylcytosine to 5-formylcytosine and 5-carboxylcytosine. *Science* 333, 1300–1303.
- (33) Pfaffeneder, T., Hackner, B., Truss, M., Munzel, M., Muller, M., Deiml, C. A., Hagemeyer, C., and Carell, T. (2011) The discovery of 5-formylcytosine in embryonic stem cell DNA. *Angew. Chem., Int. Ed.* 50, 7008–7012.
- (34) Raiber, E., Murat, P., Chirgadze, D. Y., Beraldi, D., Luisi, B. F., and Balasubramanian, S. (2015) 5-Formylcytosine alters the structure of the DNA double helix. *Nat. Struct. Mol. Biol.* 22, 44–49 DOI: 10.1038/nsmb.2936.
- (35) Stivers, J. T. (2004) Site-specific DNA damage recognition by enzyme-induced base flipping. *Prog. Nucleic Acid Res. Mol. Biol.* 77, 37–65.
- (36) Hardeland, U., Bentele, M., Lettieri, T., Steinacher, R., Jiricny, J., and Schar, P. (2001) Thymine DNA glycosylase. *Prog. Nucleic Acid Res. Mol. Biol.* 68, 235–253.
- (37) Hashimoto, H., Zhang, X., and Cheng, X. (2013) Selective excision of 5-carboxylcytosine by a thymine DNA glycosylase mutant. *J. Mol. Biol.* 425, 971–976.
- (38) Wing, R., Drew, H., Takano, T., Broka, C., Tanaka, S., Itakura, K., and Dickerson, R. E. (1980) Crystal structure analysis of a complete turn of B-DNA. *Nature* 287, 755–758.

- (39) Drew, H. R., Wing, R. M., Takano, T., Broka, C., Tanaka, S., Itakura, K., and Dickerson, R. E. (1981) Structure of a B-DNA dodecamer: conformation and dynamics. *Proc. Natl. Acad. Sci. U.S.A.* 78, 2179–2183.
- (40) Tereshko, V., Minasov, G., and Egli, M. (1999) The Dickerson–Drew B-DNA dodecamer revisited at atomic resolution. *J. Am. Chem. Soc.* 121, 470–471.
- (41) Howerton, S. B., Sines, C. C., VanDerveer, D., and Williams, L. D. (2001) Locating monovalent cations in the grooves of B-DNA. *Biochemistry* 40, 10023–10031.
- (42) Kowal, E. A., Ganguly, M., Pallan, P. S., Marky, L. A., Gold, B., Egli, M., and Stone, M. P. (2011) Altering the electrostatic potential in the major groove: thermodynamic and structural characterization of 7-deaza-2'-deoxyadenosine:dT base pairing in DNA. *J. Phys. Chem. B* 115, 13925–13934.
- (43) Kowal, E. A., Lad, R. R., Pallan, P. S., Dhummakupt, E., Wawrzak, Z., Egli, M., Sturla, S. J., and Stone, M. P. (2013) Recognition of *O*⁶-benzyl-2'-deoxyguanosine by a perimidinone-derived synthetic nucleoside: a DNA interstrand stacking interaction. *Nucleic Acids Res.* 41, 7566–7576.
- (44) Hare, D. R., Wemmer, D. E., Chou, S. H., Drobny, G., and Reid, B. R. (1983) Assignment of the non-exchangeable proton resonances of d(C-G-C-G-A-A-T-T-C-G-C-G) using two-dimensional nuclear magnetic resonance methods. *J. Mol. Biol.* 171, 319–336.
- (45) Moe, J. G., and Russu, I. M. (1990) Proton exchange and base-pair opening kinetics in 5'-d(CGCGAATTCGCG)-3' and related dodecamers. *Nucleic Acids Res.* 18, 821–827.
- (46) Tjandra, N., Tate, S.-I., Ono, A., Kainosho, M., and Bax, A. (2000) The NMR structure of a DNA dodecamer in an aqueous dilute liquid crystalline phase. *J. Am. Chem. Soc.* 122, 6190–6200.
- (47) Singh, S. K., Szulik, M. W., Ganguly, M., Khutsishvili, I., Stone, M. P., Marky, L. A., and Gold, B. (2011) Characterization of DNA with an 8-oxoguanine modification. *Nucleic Acids Res.* 39, 6789–6801.
- (48) Cavaluzzi, M. J., and Borer, P. N. (2004) Revised UV extinction coefficients for nucleoside-5'-monophosphates and unpaired DNA and RNA. *Nucleic Acids Res.* 32, e13.
- (49) Marky, L. A., and Breslauer, K. J. (1987) Calculating thermodynamic data for transitions of any molecularity from equilibrium melting curves. *Biopolymers* 26, 1601–1620.
- (50) Bodenhausen, G., Wagner, G., Rance, M., Sorensen, O. W., Wuthrich, K., and Ernst, R. R. (1984) Longitudinal two-spin order in 2D exchange spectroscopy (NOESY). *J. Magn. Reson.* 59, 542–550.
- (51) Piotto, M., Saudek, V., and Sklenar, V. (1992) Gradient-tailored excitation for single-quantum NMR spectroscopy of aqueous solutions. *J. Biomol. NMR* 6, 661–665.
- (52) Chen, C., and Russu, I. M. (2004) Sequence-dependence of the energetics of opening of at basepairs in DNA. *Biophys. J.* 87, 2545–2551.
- (53) Chen, C., Jiang, L., Michalczyk, R., and Russu, I. M. (2006) Structural energetics and base-pair opening dynamics in sarcin-ricin domain RNA. *Biochemistry* 45, 13606–13613.
- (54) Huang, Y., Chen, C., and Russu, I. M. (2009) Dynamics and stability of individual base pairs in two homologous RNA–DNA hybrids. *Biochemistry* 48, 3988–3997.
- (55) Huang, Y., Weng, X., and Russu, I. M. (2010) Structural energetics of the adenine tract from an intrinsic transcription terminator. *J. Mol. Biol.* 397, 677–688.
- (56) Huang, Y., Weng, X., and Russu, I. M. (2011) Enhanced base-pair opening in the adenine tract of a RNA double helix. *Biochemistry* 50, 1857–1863.
- (57) Gueron, M., and Leroy, J. L. (1995) Studies of base pair kinetics by NMR measurement of proton exchange. *Methods Enzymol.* 261, 383–413.
- (58) Szulik, M. W., Voehler, M., and Stone, M. P. (2014) NMR analysis of base-pair opening kinetics in DNA. *Curr. Prot. Nucl. Acid Chem.* 59, 7.20.1–7.20.18 DOI: 10.1002/0471142700.nc0720s59.
- (59) Plateau, P., and Gueron, M. (1982) Exchangeable proton NMR without base-line distortion, using new strong-pulse sequences. *J. Am. Chem. Soc.* 104, 7310–7311.
- (60) Crenshaw, C. M., Wade, J. E., Arthanari, H., Frueh, D., Lane, B. F., and Nunez, M. E. (2011) Hidden in plain sight: subtle effects of the 8-oxoguanine lesion on the structure, dynamics, and thermodynamics of a 15-base pair oligodeoxynucleotide duplex. *Biochemistry* 50, 8463–8477.
- (61) Parker, J. B., and Stivers, J. T. (2011) Dynamics of uracil and 5-fluorouracil in DNA. *Biochemistry* 50, 612–617.
- (62) Rosenbaum, G., Alkire, R. W., Evans, G., Rotella, F. J., Lazarski, K., Zhang, R. G., Ginell, S. L., Duke, N., Naday, I., Lazarz, J., Molitsky, M. J., Keefe, L., Gonczy, J., Rock, L., Sanishvili, R., Walsh, M. A., Westbrook, E., and Joachimiak, A. (2006) The Structural Biology Center 19ID undulator beamline: facility specifications and protein crystallographic results. *J. Synchrotron Radiat.* 13, 30–45.
- (63) Minor, W., Cymborowski, M., Otwinowski, Z., and Chruszcz, M. (2006) HKL-3000: the integration of data reduction and structure solution—from diffraction images to an initial model in minutes. *Acta Crystallogr., Sect. D: Biol. Crystallogr.* 62, 859–866.
- (64) Kabsch, W. (2010) Integration, scaling, space-group assignment and post-refinement. *Acta Crystallogr., Sect. D: Biol. Crystallogr.* 66, 133–144.
- (65) Kabsch, W. (2010) XDS. *Acta Crystallogr., Sect. D: Biol. Crystallogr.* 66, 125–132.
- (66) Evans, P. (2006) Scaling and assessment of data quality. *Acta Crystallogr., Sect. D: Biol. Crystallogr.* 62, 72–82.
- (67) Collaborative Computational Project Number 4 (1994) The CCP4 suite: Programs for protein crystallography. *Acta Crystallogr., Sect. D: Biol. Crystallogr.* 50, 760–763.
- (68) Otwinowski, Z., and Minor, W. (1997) Processing of X-ray diffraction data collected in oscillation mode. *Acta Crystallogr., Sect. A* 276, 307–326.
- (69) Vagin, A. (1989) New translation and packing functions, in *Newsletter on Protein Crystallography*, Vol. 24, pp 117–121, Daresbury Laboratory.
- (70) Vagin, A., and Teplyakov, A. (1997) MOLREP: an automated program for molecular replacement. *J. Appl. Crystallogr.* 30, 1022–1025.
- (71) Emsley, P., Lohkamp, B., Scott, W. G., and Cowtan, K. (2010) Features and development of Coot. *Acta Crystallogr., Sect. D: Biol. Crystallogr.* 66, 486–501.
- (72) Winn, M. D., Murshudov, G. N., and Papiz, M. Z. (2003) Macromolecular TLS refinement in REFMAC at moderate resolutions. *Methods Enzymol.* 374, 300–321.
- (73) Vagin, A. A., Steiner, R. A., Lebedev, A. A., Potterton, L., McNicholas, S., Long, F., and Murshudov, G. N. (2004) REFMAC5 dictionary: organization of prior chemical knowledge and guidelines for its use. *Acta Crystallogr., Sect. D: Biol. Crystallogr.* 60, 2184–2195.
- (74) Boelens, R., Scheek, R. M., Dijkstra, K., and Kaptein, R. (1985) Sequential assignment of imino- and amino-proton resonances in ¹H NMR spectra of oligonucleotides by two-dimensional NMR spectroscopy. Application to a lac operator fragment. *J. Magn. Reson.* 62, 378–386.
- (75) Russu, I. M. (2004) Probing site-specific energetics in proteins and nucleic acids by hydrogen exchange and nuclear magnetic resonance spectroscopy. *Methods Enzymol.* 379, 152–175.
- (76) Every, A. E., and Russu, I. M. (2008) Influence of magnesium ions on spontaneous opening of DNA base pairs. *J. Phys. Chem. B* 112, 7689–7695.
- (77) Huang, Y. G., Chen, C. J., and Russu, I. M. (2009) Structural energetics of a DNA–RNA hybrid containing a tract of dA–rU base pairs. *J. Biomol. Struct. Dyn.* 26, 900–900.
- (78) Kopka, M. L., Fratini, A. V., Drew, H. R., and Dickerson, R. E. (1983) Ordered water structure around a B-DNA dodecamer. A quantitative study. *J. Mol. Biol.* 163, 129–146.
- (79) Patel, D. J., Shapiro, L., and Hare, D. (1987) DNA and RNA: NMR studies of conformations and dynamics in solution. *Q. Rev. Biophys.* 20, 35–112.
- (80) Reid, B. R. (1987) Sequence-specific assignments and their use in NMR studies of DNA structure. *Q. Rev. Biophys.* 20, 2–28.

- (81) Sumino, M., Ohkubo, A., Taguchi, H., Seio, K., and Sekine, M. (2008) Synthesis and properties of oligodeoxynucleotides containing 5-carboxy-2'-deoxycytidines. *Bioorg. Med. Chem. Lett.* 18, 274–277.
- (82) Burdzy, A., Noyes, K. T., Valinluck, V., and Sowers, L. C. (2002) Synthesis of stable-isotope enriched 5-methylpyrimidines and their use as probes of base reactivity in DNA. *Nucleic Acids Res.* 30, 4068–4074.
- (83) Lau, A. Y., Scharer, O. D., Samson, L., Verdine, G. L., and Ellenberger, T. (1998) Crystal structure of a human alkylbase-DNA repair enzyme complexed to DNA: mechanisms for nucleotide flipping and base excision. *Cell* 95, 249–258.
- (84) Parikh, S. S., Mol, C. D., Hosfield, D. J., and Tainer, J. A. (1999) Envisioning the molecular choreography of DNA base excision repair. *Curr. Opin. Struct. Biol.* 9, 37–47.
- (85) Bruner, S. D., Norman, D. P., and Verdine, G. L. (2000) Structural basis for recognition and repair of the endogenous mutagen 8-oxoguanine in DNA. *Nature* 403, 859–866.
- (86) Hollis, T., Ichikawa, Y., and Ellenberger, T. (2000) DNA bending and a flip-out mechanism for base excision by the helix-hairpin-helix DNA glycosylase, *Escherichia coli* AlkA. *EMBO J.* 19, 758–766.
- (87) Tainer, J. A. (2001) Structural implications of BER enzymes: dragons dancing—the structural biology of DNA base excision repair. *Prog. Nucleic Acid Res. Mol. Biol.* 68, 299–304.
- (88) Fromme, J. C., Banerjee, A., and Verdine, G. L. (2004) DNA glycosylase recognition and catalysis. *Curr. Opin. Struct. Biol.* 14, 43–49.
- (89) Fromme, J. C., and Verdine, G. L. (2004) Base excision repair. *Adv. Protein Chem.* 69, 1–41.
- (90) Cao, C., Jiang, Y. L., Stivers, J. T., and Song, F. (2004) Dynamic opening of DNA during the enzymatic search for a damaged base. *Nat. Struct. Mol. Biol.* 11, 1230–1236.
- (91) Krosky, D. J., Song, F., and Stivers, J. T. (2005) The origins of high-affinity enzyme binding to an extrahelical DNA base. *Biochemistry* 44, 5949–5959.
- (92) Parker, J. B., Bianchet, M. A., Krosky, D. J., Friedman, J. I., Amzel, L. M., and Stivers, J. T. (2007) Enzymatic capture of an extrahelical thymine in the search for uracil in DNA. *Nature* 449, 433–437.
- (93) Friedman, J. I., and Stivers, J. T. (2010) Detection of damaged DNA bases by DNA glycosylase enzymes. *Biochemistry* 49, 4957–4967.
- (94) Karino, N., Ueno, Y., and Matsuda, A. (2001) Synthesis and properties of oligonucleotides containing 5-formyl-2'-deoxycytidine: *in vitro* DNA polymerase reactions on DNA templates containing 5-formyl-2'-deoxycytidine. *Nucleic Acids Res.* 29, 2456–2463.
- (95) Kamiya, H., Tsuchiya, H., Karino, N., Ueno, Y., Matsuda, A., and Harashima, H. (2002) Mutagenicity of 5-formylcytosine, an oxidation product of 5-methylcytosine, in DNA in mammalian cells. *J. Biochem.* 132, 551–555.
- (96) Hashimoto, H., Liu, Y., Upadhyay, A. K., Chang, Y., Howerton, S. B., Vertino, P. M., Zhang, X., and Cheng, X. (2012) Recognition and potential mechanisms for replication and erasure of cytosine hydroxymethylation. *Nucleic Acids Res.* 40, 4841–4849.
- (97) Maiti, A., Morgan, M. T., and Drohat, A. C. (2009) Role of two strictly conserved residues in nucleotide flipping and N-glycosylic bond cleavage by human thymine DNA glycosylase. *J. Biol. Chem.* 284, 36680–36688.
- (98) Jang, H., Shin, H., Eichman, B. F., and Huh, J. H. (2014) Excision of 5-hydroxymethylcytosine by DEMETER family DNA glycosylases. *Biochem. Biophys. Res. Commun.* 446, 1067–1072.
- (99) Brooks, S. C., Fischer, R. L., Huh, J. H., and Eichman, B. F. (2014) 5-Methylcytosine recognition by *Arabidopsis thaliana* DNA glycosylases DEMETER and DML3. *Biochemistry* 53, 2525–2532.